A Semi-Implicit Method for the Analysis of Two-Dimensional Fluid Flow with Moving Free Surfaces

Jong Sun Park
School of Mechanical and Aerospace Engineering, Seoul National University, Seoul 151-742, Korea
Min Soo Kim
MEMS Lab., Samsung Advanced Institute of Technology, Suwon 440-600, Korea
Joon Sik Lee, Woo Il Lee*
School of Mechanical and Aerospace Engineering, Seoul National University, Seoul 151-742, Korea

Flow with moving free surfaces is analyzed with an the Eulerian coordinate system. This study proposes a semi-implicit filling algorithm using VOF in which the PLIC (Piecewise Linear Interface Calculation)-type interface reconstruction method and the donor-acceptor -type front advancing scheme are adopted. Also, a new scheme using extrapolation of the stream function is proposed to find the velocity of the node that newly enters the computational domain. The effect of wall boundary conditions on the flow field and temperature field is examined by numerically solving a two-dimensional casting process.

Key Words : Free Surface, Fixed Grid System, Volume of Fluid (VOF) method, Mold Filling Process, Fractional Step Method, Wall Boundary Condition Nomenclature

Nomenclature

A_j : Area of the j-th face
c_p : Specific heat
$\mathbf{C}(\mathbf{u})$: Convection matrix
$D_e^{(k)}$: Divergence of element
f : Volume fraction of element
$\mathbf{F}$: Force matrix
h : Heat transfer coefficient
$\boldsymbol{H}$: Pressure gradient matrix
$\boldsymbol{h_e}$: Pressure gradient matrix of element
$\boldsymbol{h_e}^T$: Divergence operator of element
$\boldsymbol{K}$: Diffusion matrix
k : Thermal conductivity
$\boldsymbol{M}$: Mass matrix
$\boldsymbol{m_e}$: Mass matrix of element
p : Pressure
T : Temperature
$\mathbf{u}$, u_i : Velocity vector and its component
V_i : Volume of the i-th element

Greek Letters

μ : Viscosity
ρ : Density
σ_{ij} : Viscous stress tensor
Ψ : Stream function

Superscripts

T : Transpose
n : Time step
(k) : Iteration number

Subscripts

e : Element
i : Cell number
$inlet$: Inlet
j : Face number

* Corresponding Author,
E-mail : wilee@snu.ac.kr
TEL : +82-2-880-7116; **FAX** : +82-2-883-0179
School of Mechanical and Aerospace Engineering, Seoul National University, San 56-1, Shinlim-dong, Kwanak-ku, Seoul 151-742, Korea. (Manuscript **Received** October 13, 2001; **Revised** January 28, 2002)

1. Introduction

Viscous flow with moving free surfaces poses a moving boundary problem where the domain has an unknown boundary which has to be deter-

mined as a part of the solution procedure. Identification and treatment of this problem are important in many technological applications such as casting of metal, injection molding of plastics, glass forming processes, formation of micro droplets, and so on. The great difficulty in treating this problem is due to continuous change of the domain and the physical discontinuity of the interface. The available approaches to the moving boundary problem can be categorized in general as Lagrangian, Eulerian, and ALE (Arbitrary Lagrangian-Eulerian). In the Lagrangian method, the coordinate system moves with the same velocity as the fluid, and as a result, the material interfaces can be precisely followed and the boundary conditions on the interface can be applied with accuracy. However, the flow with large deformation and complex geometry may cause distortion and tangling of the mesh. In that case, rezoning or reconnection of the distorted mesh is inevitable. The Eulerian methods are characterized by the fixed coordinate system through which the fluid moves. Using the fixed grid system, it is easy to efficiently deal with flow that undergoes large motion and to extend two-dimensional codes to three-dimension. On the other hand, a special scheme is necessary to accurately locate the interface without loss of sharp discontinuity, because the interface does not coincide with the grid points but moves through them. Frequently used methods include VOF (Volume of Fluid) method (Hirt and Nichols, 1981), MAC (Marker And Cell) method (Harlow and Welch, 1965), SLIC (Simple Line Interface Calculation) method (Noh and Woodward, 1976), and Young's method (Young, 1982). Considering the efficiency of calculations and the availability in complex flows, VOF method is adopted in this study and a semi-implicit front-advancing algorithm is proposed.

In the analysis of non-isothermal flow with free boundary, the velocity boundary conditions at the solid wall directly affect the development of both velocity and thermal boundary layers, largely affecting the overall accuracy of the calculation. Among the common forms of wall boundary conditions, there are the no-slip condition, the free-slip condition, and the slip condition with shear stress depending on the relative magnitude of the boundary layer thickness and mesh size. However, due to the restricted power of computers, many researchers have applied the shear-stress boundary condition on a relatively coarse grid. To demonstrate the effects of the wall boundary conditions on the overall calculation results, this study compares the calculation results from the case of applying the no-slip boundary condition and the slip boundary condition with shear stress.

2. Incompressible Fluid Flow and Fractional Step Method

2.1 Governing equations and fractional step method

The governing equations for laminar incompressible Newtonian fluids are the continuity equation and the unsteady Navier-Stokes equations described as follows;

$$\rho(\dot{u}_i+u_ju_{i,j})=-p_{,i}+\sigma_{ij,j}+f_i \tag{1}$$

$$u_{i,i}=0 \tag{2}$$

where $\sigma_{ij}=\mu(u_{i,j}+u_{j,i})$ and ρ is the density. u_i and p are the velocity and the pressure, respectively. f_i is the body force. The energy conservation equation is also included in the governing equations.

$$\rho c_p(\dot{T}+u_jT_{,j})=kT_{,ii} \tag{3}$$

Here, T is the temperature and c_p and k are the specific heat and the thermal conductivity of the fluid, respectively. The thermal boundary condition for the above equation may be the essential condition or the convection heat transfer condition;

$$T=T_{inlet} \tag{4}$$

$$q=h(T-T_\infty) \tag{5}$$

where h is the convection heat transfer coefficient and T_{inlet} and T_∞ denote the inlet and surrounding temperature, respectively.

Chorin (1968) first proposed a fractional step method on the finite difference framework and Donea et al. (1982), Ramaswamy (1988), Ramaswamy and Jue (1992), and De Sampaio (1991)

applied the method on the finite element framework. Mizukami and Tsuchiya (1984), Kawahara and Ohmiya (1985) and Nakayama and Mori (1996) studied the flow with moving free surfaces using the fractional step method. This method takes the fractional step approach to the numerical time integration of the unsteady Navier-Stokes equations so that only the continuity equation and the pressure terms are treated in an implicit manner. Then, the intermediate velocity which satisfies only the momentum equation and does not necessarily meet the continuity constraint, is adjusted by the pressure to meet the divergence-free condition. This reflects the dual role of pressure; one is the pressure force in the momentum equation, and the other is an implicit one that enforces the divergence-free constraint in incompressible flow.

2.2 Explicit element-by-element fractional step method

Nakayama and Mori (1996) proposed the explicit element-by-element fractional step method and Kim et al. (2000 a, b) applied it in analyzing mold filling processes and the sloshing problems. The semi-discretized momentum equations and the continuity equation can be written as

$$\mathbf{M}\dot{\mathbf{u}}+\mathbf{C}(\mathbf{u})\mathbf{u}+\mathbf{K}\mathbf{u}-\mathbf{H}\mathbf{p}-\mathbf{F}=\mathbf{0} \tag{6}$$

$$\mathbf{h}_e{}^T\mathbf{u}_e=0 \quad (d=1, 2, 3, \cdots, NE) \tag{7}$$

where $\mathbf{u}$ and $\mathbf{p}$ are the nodal velocity and pressure vectors, respectively. $\mathbf{M}$, $\mathbf{C}(\mathbf{u})$, $\mathbf{K}$ and $\mathbf{H}$ are the mass, convection, diffusion and pressure gradient matrix. Also, $\mathbf{F}$ is the force vector, $\mathbf{h}_e{}^T$ is the divergence matrix of the element and NE is the number of elements. In this formulation, a bilinear shape function is applied for the velocity variable and an element-wise constant shape function for the pressure variable. In the time-integration of the semi-discretized Navier-Stokes equations, an explicit scheme is employed except for the pressure force term. Subsequently, the implicit fractional-step time-integration for the pressure leads to the following equations;

$$D_e{}^{(k)}=\frac{1}{V_e}\mathbf{h}_e{}^T\mathbf{u}_e{}^{n+1,(k)} \tag{8}$$

$$p_e{}^{n+1,(k+1)}=p_e{}^{n+1,(k)}+\Delta p_e{}^{n+1,(k)} \tag{9}$$

$$\Delta p_e{}^{n+1,(k)}=-\lambda_e D_e{}^{(k)} \tag{10}$$

$$\lambda_e=\frac{V_e}{\Delta t\mathbf{h}_e{}^T\mathbf{m}_e{}^{-1}\mathbf{h}_e} \tag{11}$$

$$\mathbf{u}_e{}^{n+1,(k+1)}=\mathbf{u}_e{}^{n+1,(k)}+\Delta t^n\mathbf{m}_e{}^{-1}\mathbf{h}_e\Delta p_e{}^{n+1,(k)} \tag{12}$$

where the superscripts $(n+1)$ and (k) denote the time step and the iteration number, respectively. $D_e{}^{(k)}$ is the local divergence of element and V_e is the volume of the element. $\mathbf{h}_e$ and $\mathbf{m}_e{}^{-1}$ are the element matrix of $\mathbf{H}$ and $\mathbf{M}^{-1}$, respectively. This study applies the constraint of mass conservation not on the global mesh but on each element. That is, the steps of pressure correction (Eq. (9)) and velocity correction (Eq. (12)) are performed for each element until the divergence of each element $D_e{}^{(k)}$ is within the convergence criterion.

This study adopts the consistent streamline upwind/Petrov-Galerkin (SUPG) formulation (Brooks and Hughes, 1982) as the upwind scheme. This formulation adds a streamline upwind perturbation (or diffusion) to the weighting function that acts only in the flow direction. The modified weighting function is applied to all terms in the momentum equations.

3. Analysis of Flow with Free Surfaces Using a Fixed Coordinate System

3.1 VOF method

VOF method was first developed by Hirt and Nichols (1981) and is the representative algorithm for solving flows with moving free surfaces on a fixed coordinate system. The volume of fluid f is defined as the volume fraction of a fluid in an element. Movement of the interface is represented by the following transport equation of f :

$$\frac{\partial f}{\partial t}+\nabla\cdot(\mathbf{u}f)=0 \tag{13}$$

This equation has only the advection term, so the solution by direct discretization is apt to cause severe numerical smearing of the flow front. To circumvent this problem, the donor-acceptor method was proposed by Ramshaw and Trapp (1976). Recently, Rider and Kothe (1998), Harvie and Fletcher (2000), and Gueyffier et al. (1999) proposed a scheme to advance the flow

front using the geometric and lagrangian aspects of the VOF transport equation. Also, Harvie and Fletcher (2001) used the stream function in updating the flow field.

3.2 Semi-implicit VOF method

The coupling between the VOF field and the velocity field makes the problem fully implicit in nature. In this study, however, those fields are decoupled and the explicit scheme is applied. Integration of Eq. (13) for the control volume results in

$$\frac{\partial f}{\partial t}V_i+\int_{\Gamma}(\mathbf{u}\cdot\mathbf{n})\,f d\Gamma=0 \tag{14}$$

where Γ denotes the boundary of the domain. Then, application of the explicit method and the Crank-Nicolson method in time integration yields

$$f_i^{n+1}=f_i^n+\frac{\Delta t}{V_i}\left[-\sum_j(\mathbf{u}^n\cdot\mathbf{n})\,f_{\Gamma_j}{}^nA_j\right] \tag{15}$$

$$\begin{aligned}f_i^{n+1}&=f_i^n+\frac{\Delta t}{V_i}\left[-\sum_j(\mathbf{u}^{n+1/2}\cdot\mathbf{n})\,f_{\Gamma_j}{}^{n+1/2}A_j\right]\\&=f_i^n+\frac{\Delta t}{V_i}\left[-\sum_j\frac{(\mathbf{u}^n+\mathbf{u}^{n+1})\cdot\mathbf{n}}{2}\,\frac{f_{\Gamma_j}{}^n+f_{\Gamma_j}{}^{n+*}}{2}A_j\right]\end{aligned} \tag{16}$$

$$f_i^{n+*}=f_i^n+\frac{\Delta t}{V_i}\left[-\sum_j(\mathbf{u}^{n+1}\cdot\mathbf{n})\,f_{\Gamma_j}{}^nA_j\right] \tag{17}$$

and

$$f_{\Gamma_j}\equiv\frac{A_j^{wet}}{A_j} \tag{18}$$

where the subscripts i and j represent the cell and the face number, respectively. A_j is the area of the j-th face, A_j^{wet} is the wetted area of A_j (see Fig. 1(a)), and the wet-out fraction f_{Γ_j} is defined as the ratio of the two. As in Fig. 1(b), f^{n+*} is the f distribution after advection of f^n with velocity $\mathbf{u}^{n+1}$. Also, $f_{\Gamma_j}{}^{n+*}$ and $f_{\Gamma_j}{}^n$ are the wet-out fractions based on f^{n+*} and f^n distributions, respectively. The calculation time used in the semi-implicit update (Eqs. (16)~(17)) of the flow front is about twice the time used in the explicit one (Eq. (15)). However, the portion of the calculation time used in the advancement of the flow front is relatively very small, so the load added to the overall calculation by the semi-implicit scheme is minimal. Furthermore, the accuracy is raised to the second order with respect to time.

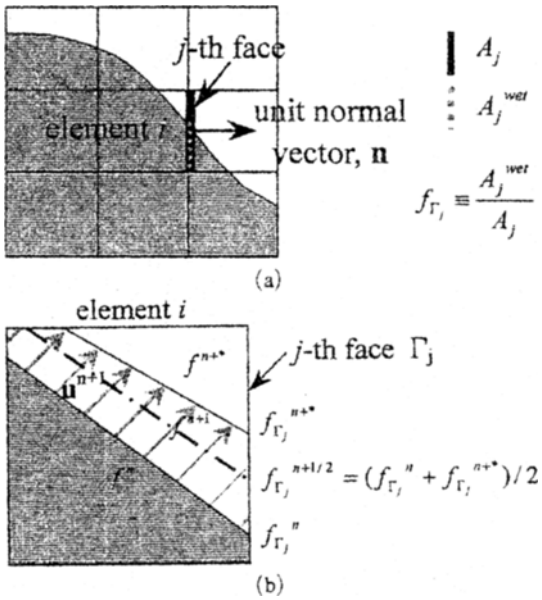

Fig. 1 Definition sketches: (a) the definition of the wet-out fraction f_{Γ_j}; (b) the wet-out fraction $f_{\Gamma_j}{}^{n+1/2}$ used in the semi-implicit scheme

3.3 Determination of the wet-out fraction f_{Γ_j}

The algorithm to calculate the wet-out fractions $f_{\Gamma_j}{}^n$ and $f_{\Gamma_j}{}^{n+*}$ from the distribution of f^n and f^{n+*} is based on the baby-cell method of Kim et al. (2000a), which utilizes the PLIC-type representation of the free surface within elements. The orientation vector $\mathbf{r}$ is defined inside an element as

$$\mathbf{r}=\frac{\sum_j(f_{ij}\cdot V_{ij})\,a_j\mathbf{n}_j}{\left|\sum_j(f_{ij}\cdot V_{ij})\,a_j\mathbf{n}_j\right|} \tag{19}$$

where f_{ij} and V_{ij} represent the volume-of-fluid and the volume of the element adjacent to the j-th face of the i-th element, respectively. Also, $\mathbf{n}_j$ is the outward unit vector normal to the element boundary Γ_j and a_j is the ratio of the j-th face area to the total peripheral area of the i-th element. The orientation vector is determined by averaging the volume-of-fluid of the neighboring elements and is a unit vector indicating

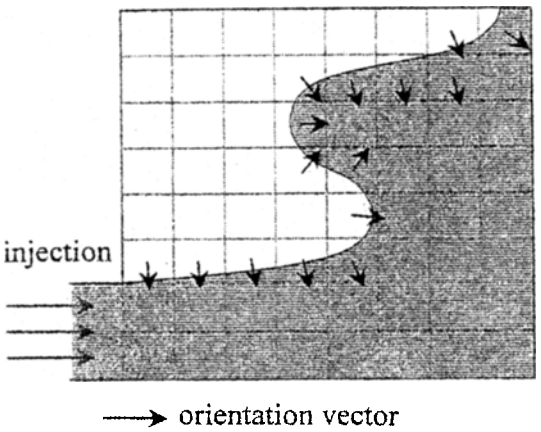

Fig. 2 Schematic representation of orientation vectors at the free surface elements

the direction where fluid is abundant, as shown in Fig. 2. The orientation vector is utilized to determine the wet-out fraction in the following manner:

(1) A plane, which is normal to the orientation vector r, and passed through the centroid of an element, is generated (see Fig. 3 (a)).

(2) Each element is discretized by baby-cells with equal area (see Fig. 3 (b)).

(3) Baby-cells are filled up in a sequence beginning with a cell which is the farthest from the plane in the positive direction of the orientation vector, **r**. Then, wet-out fractions of the element can be calculated (see Fig. 3 (c)).

3.4 Wall boundary conditions

Commonly used boundary conditions on the wall can be classified as follows;

$$\text{no-slip condition} \quad : u_i = b_i \tag{20}$$

$$\text{slip condition} \quad : u_i n_i = 0,\ \sigma_t = 0 \tag{21}$$

$$\text{shear stress condition} : u_i n_i = 0,\ \sigma_t = f(u_t) = 0.5\rho u_t^2 \times 0.664/\sqrt{\mathrm{Re}_D} \tag{22}$$

where b_i is the speed of the wall and n_i denotes the normal vector to the wall. σ_t is the shear stress at the wall and the shear stress function $f(u_t)$ is based on the analytic solution of the external flow on a flat plate. Proper choice of the wall boundary condition is taken by considering the relative magnitude of the boundary layer thickness and mesh size at the wall (Gao, 1999). If the

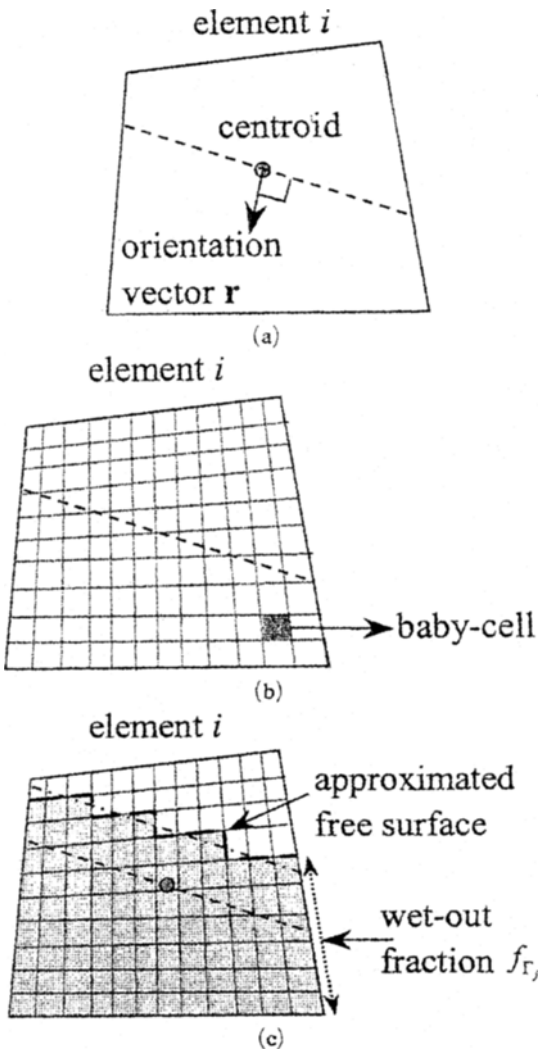

Fig. 3 Illustration of the procedure to calculate the wet-out fraction at the element boundary: (a) construct a line normal to **r**; (b) discretize the element i by the baby-cells; (c) fill up the baby-cells and calculate the wet-out fraction.

boundary layer thickness is much smaller than the mesh size at the wall, the slip boundary condition is acceptable. If the mesh size is much smaller than the boundary layer thickness, the no-slip boundary condition is proper, and if the two have an equal order of magnitude, the shear-stress boundary condition is recommendable. Most researchers (Lewis et al., 1995; Dhatt et al., 1990; Usmani et al., 1992; Hetu and Ilinica, 1999; Gao, 1999) have applied shear stress

boundary conditions and some have employed the no-slip boundary condition (Shin and Lee, 1997, 2000). In addition, Kim et al. (2000b) applied a body force equivalent to the shear stress. To study the effect of wall boundary condition, the no-slip boundary condition and the shear-stress boundary condition was used at the mold wall.

3.5 Specification of velocity at the node that newly enters the computational domain

In the calculation of flows with moving free surfaces using a fixed grid system, only the elements of which VOF is greater than 0.5 ($f>0.5$) are included in the calculation domain. Hence, when a node newly enters the calculation domain, the old-value velocity of the node is necessary (see Fig. 4). Kim et al. (2000a) and Nakayama and Mori (1996) used the volume-averaged velocity of the neighboring nodes as follows;

$$\mathbf{u}^{newnode}=\frac{\sum\bar{\mathbf{u}}_e\cdot V_e}{\sum V_e} \tag{23}$$

where $\bar{\mathbf{u}}_e$ and V_e are the average velocity and the volume of element, respectively. However, one of disadvantages of this method is that it does not guarantee the divergence-free condition. This study uses the stream function ψ that exists in two-dimensional incompressible flow. The stream function calculated by Eq. (24) is extrapolated to obtain the velocity using Eq. (25).

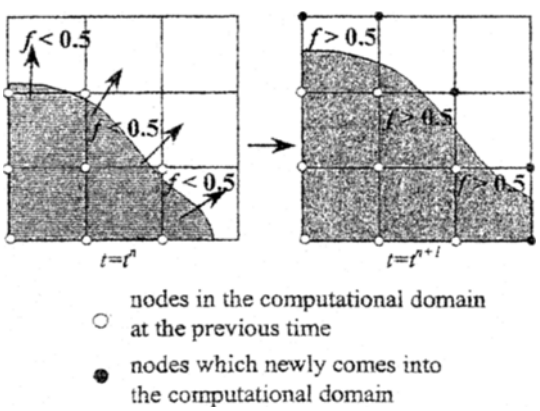

Fig. 4 Specification of the velocity value at the node which enters the computational domain at the new time step

$$\nabla^2\psi=-u_{2,1}+u_{1,2} \tag{24}$$

$$u_1=\frac{\partial\psi}{\partial x_e},\quad u_2=-\frac{\partial\psi}{\partial x_1} \tag{25}$$

The advantage of this scheme is that it satisfies the mass conservation equation more accurately. However, as a result of the fact that the stream function does not exist in the three-dimensional problem, this method is difficult to apply to the three-dimensional cases. In three-dimensional calculations, the streamline, not the stream function, can be introduced to obtain the velocity, but the larger error in divergence would obstruct practical application.

4. Results and Discussions

4.1 Verification of the code for the broken dam problem

The developed code was verified through a broken dam problem. Because both the advancing and retreating movement of the free surface can be examined in a simple geometric configuration, the broken dam problem has been a representative benchmark test for flows with moving free surfaces. As in Fig. 5, the water is contained between the wall and the gate, and with removal of the gate, the water column collapses under the effect of gravity as time proceeds. The density is 1000kg/m^3, the viscosity 1×10^{-3} Pa·s, the gravity acceleration 9.81m/s^2 and the height H is taken as 0.05175m. The numerical mesh is equi-spaced. The slip condition is specified as the boundary condition on the wall. Table 1 and

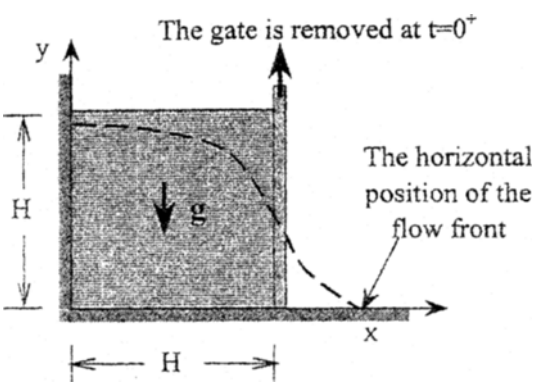

Fig. 5 Illustration of the broken dam problem

Table 1 Simulation results of the broken dam problem for different schemes

	Mesh	Front advancing Scheme	$\mathbf{u}^{newnode}$	Number of Time Step
Case A	30 * 12	Kim et al. (2000 a) : explicit scheme	Averaging of neighboring nodes	273
Case B	30 * 12	This Study : semi-implicit scheme	Extrapolation of stream function	186
Case C	48 * 19	Kim et al. (2000 a) : explicit scheme	Averaging of neighboring nodes	662
Case D	48 * 19	This Study : semi-implicit scheme	Extrapolation of stream function	326

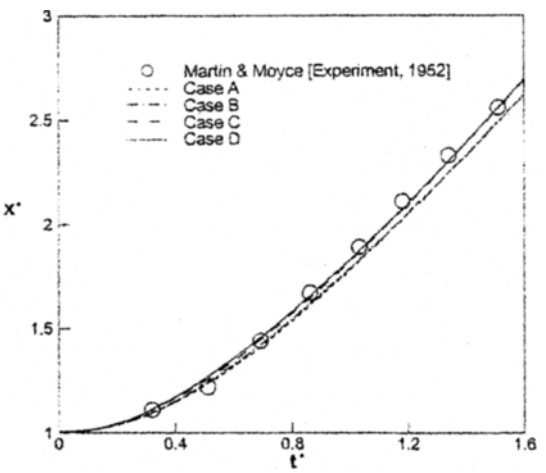

Fig. 6 Comparison of the free surface position by the numerical calculation with the experimental data (Martin and Moyce, 1952) and Kim et al. (2000a) for the broken dam problem

Fig. 6 compare the calculation results with the experiments of Martin and Moyce (1952) and the numerical analysis of Kim et al. (2000a). Here, $t^*=t\sqrt{(g/H)}$ and $x^*=x/H$ represent the dimensionless time and the position of the flow front. The result shows about the same degree of accuracy as previous studies. It should be noted that this study applies the velocity calculated from extrapolation of the stream function, while previous studies (Kim et al. 2000a) used the mean-value velocity for the node that newly enters the computational domain as in Eq. (23). On that account, the horizontal location of the flow front in this study has a slightly bigger value around $t^*=0.5$, but the overall results show good agreement between the two schemes.

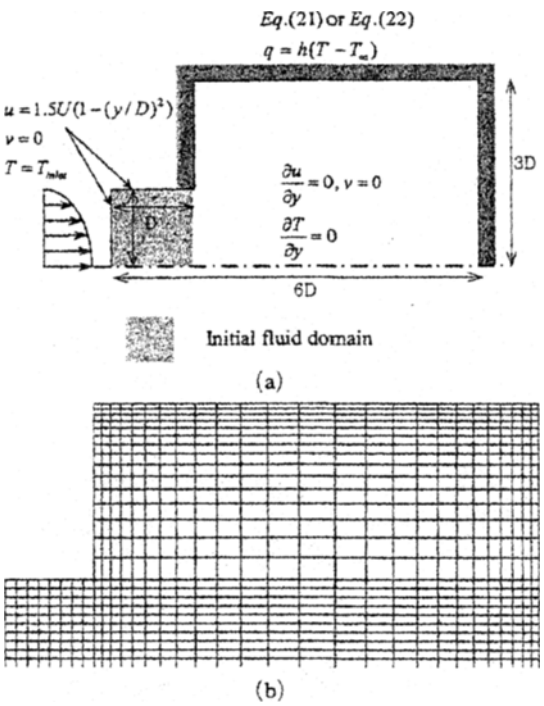

Fig. 7 Definition sketch and finite element mesh used in the analysis of mold filling process: (a) geometry and boundary conditions; (b) finite element mesh

4.2 Effect of wall boundary conditions on the analysis of mold filling process

The mold filling process was analyzed to study the effect of wall boundary condition on the velocity and temperature field. The semi-implicit scheme was adopted to advance the flow front. The geometry and boundary conditions of this comparative study are shown in Fig. 7. At the inlet, the fluid is taken to have a parabolic veloc-

ity profile. The density and viscosity of the fluid was taken as 1000kg/m^3 and 1 Pa·s, respectively. The specific heat was 900J/kg·K and the thermal conductivity was taken as 200W/m·K. The thermal boundary conditions required to solve Eq. (3) are Eqs. (4)～(5). The heat transfer coefficient was 1000W/m^2·K. The surrounding temperature T_∞ and the inlet temperature T_{inlet} was taken as 25℃ and 700℃, respectively. The average velocity at the inlet was 1m/s and a half width of the inlet was taken as 0.1m. The number of nodes is 764 and the number of elements is 705. Calculations are made for four cases with different boundary conditions at the wall, which are summarized in the Table 2.

Table 2 Minimum temperature at the end of mold filling calculated for different wall boundary conditions and schemes

	$\mathbf{u}^{newnode}$	Wall boundary condition	T_{min}(℃)
Case 1	Averaging of neighboring nodes	No-slip condition	630.1
Case 2	Extrapolation of stream function	No-slip condition	629.9
Case 3	Averaging of neighboring nodes	Shear stress condition	596.7
Case 4	Extrapolation of stream function	Shear stress condition	596.9

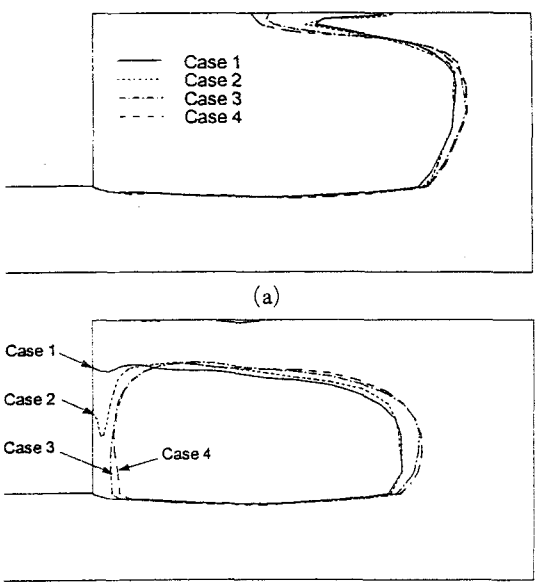

Fig. 8 Results of numerical calculation for the mold filling process. Comparison of the free surface position for the four cases: (a) t=7s; (b) t=10s.

As shown in Figs. 8 and 10, the no-slip boundary condition on the wall causes jetting of the fluid along the bottom wall. Furthermore, at the left and right sides of the upper wall arises a secondary flow (Fig. 9), and consequently the temperature field is also affected by the secondary flow. The secondary flow is assumed to occur when the flow front first reaches the middle of the wall, not the corner, as a result of the jetting flow. The velocity profile at the wall makes it clear that the mesh is inappropriate to resolve the

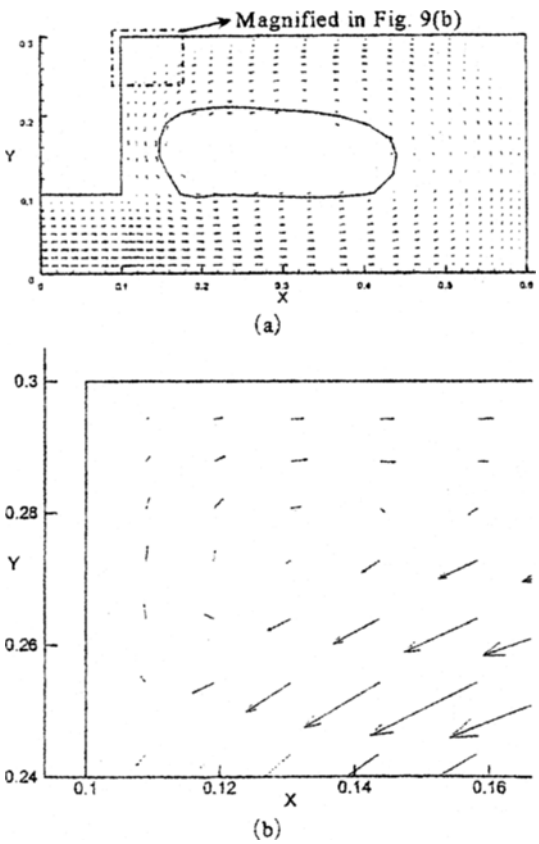

Fig. 9 Results of numerical calculation for the mold filling process: (a) overall flow pattern for Case 2 at t=12s; (b) magnified flow pattern in the upper left corner. Secondary flow is visible

development of the boundary layer at the wall by using the no-slip boundary condition. The thickness of the boundary layer for the case with the no-slip wall boundary condition on the coarse grid system is much greater than the case with the shear-stress wall boundary condition. Considering the fact that the mold filling process usually comes to an end before the boundary layer fully develops at the wall, the no-slip boundary condition is not acceptable except for the very fine grid system. Cases 3 and 4 that applied the shear-stress boundary condition show the faster advancing flow fronts than those of Cases 1 and 2 that adopted the no-slip boundary condition. Also, the flow front of Case 2 and Case 4 slightly exceeds that of Case 1 and Case 3, respectively. This was to be expected since the velocity $\mathbf{u}^{newnode}$, which was predicted by using the extrapolation of the stream function, was slightly bigger than that assumed by averaging the velocities of neighboring nodes.

As in Fig. 11, the temperature field is affected by the velocity field. In Case 1 and Case 2, the isothermal line is distorted along the stream line at the right and left corners of the upper wall under the influence of the secondary flow, while in Case 3 and Case 4, greater convective mixing with the main stream around the inlet results in

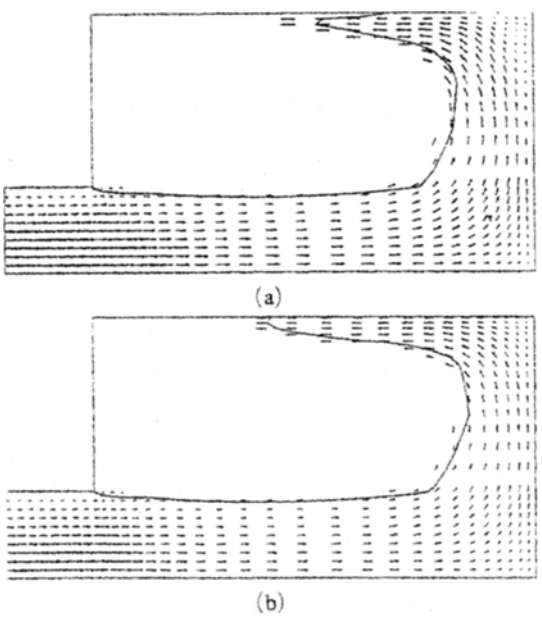

Fig. 10 Results of numerical calculation for the mold filling process. Velocity vectors and free surface positions: (a) Case 1, t=7s; (b) Case 4, t=7s

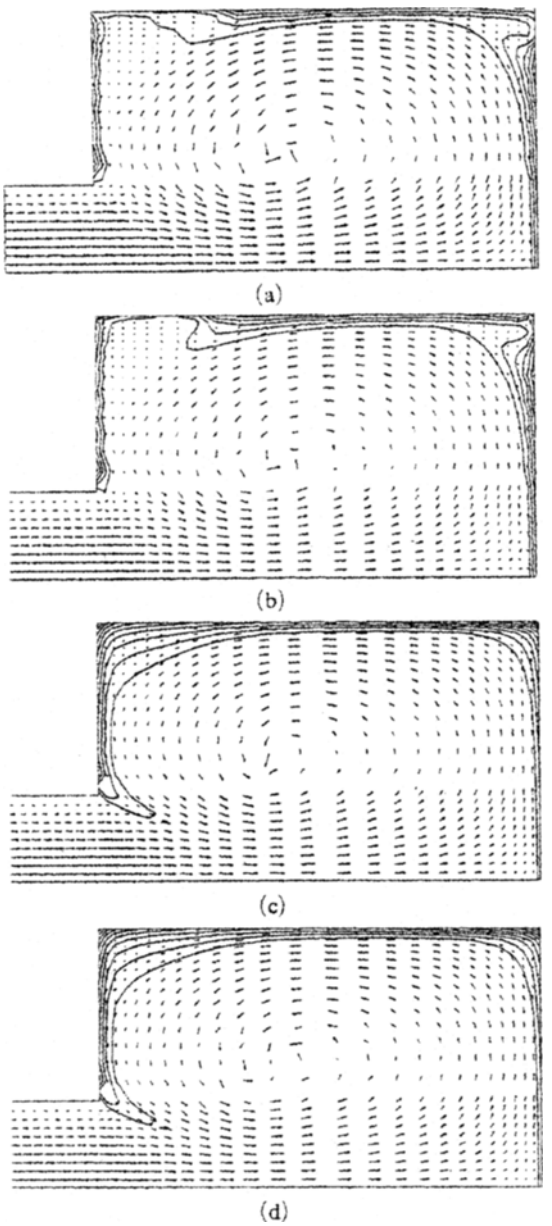

Fig. 11 Results of numerical calculation for the mold filling process at t=15s (final time). Temperature field at an equal interval of 10℃ from 600℃ to 700℃ : (a) Case 1; (b) Case 2; (c) Case 3; (d) Case 4; (e) Case 5; (f) Case 6

smoother contour lines. As can be seen in Table 2, the minimum temperature at the end of the filling process clearly shows the effect of different wall boundary conditions. The minimum temperatures for Case 3 and Case 4 are lower than those of Case 1 and Case 2. This is the result of the larger convective heat transfer caused by the slip condition at the mold wall.

The minimum mesh size at the wall in this problem is 0.0058m, and the boundary layer thickness is $\delta \cong 0.0577$m based on the analytic solution of the laminar flow on the flat plate when fully developed. However, the developing flow is supposed to have a much thinner boundary layer. Hence, for the analysis of mold filling problems, the no-slip boundary condition are not always guaranteed to give better results than the shear-stress boundary condition even when the mesh is a little fine.

5. Conclusions

In this paper, a volume-tracking algorithm based on the VOF method is presented for the analysis of the flow with moving free surfaces. This study proposed a semi-implicit scheme to advance the flow front. For ease of satisfying the divergence-free constraint, the stream function was adopted to designate the velocity of the nodes which were newly incorporated into the computational domain. Comparative studies were conducted for several problems to demonstrate the accuracy and characteristics of the proposed algorithm. Close agreement with other numerical results and experimental data was obtained.

To examine the effect of wall boundary conditions on the flow with moving free surface, a comparative study was performed on the mold filling process for different conditions. The minimum temperatures in case that applied shear-stress boundary condition were lower than those of no-slip boundary condition, which was caused by the larger convective heat transfer at the mold wall.

Acknowledgments

This work was supported by the Brain Korea-21 project and by the Korean Ministry of Science and Technology through the National Laboratory Project.

References

Brooks, A. N. and Hughes, T. J. R., 1982, "Streamline Upwind/Petrov-Galerkin Formulations for Convection Dominated Flows with Particular Emphasis on the Incompressible Navier-Stokes Equations," *Comput. Methods Appl. Mech. Engrg.*, Vol. 32, pp. 199~259.

Chorin, A. J., 1968, "Numerical Solution of the Navier-Stokes Equations," *Math. Comput.*, Vol. 22, pp. 745~762.

De Sampaio, P. A. B., 1991, "A Petrov-Galerkin Formulation for the Incompressible Navier-Stokes Equations using Equal Order Interpolation for Velocity and Pressure," *Int. J. Numer. Methods Engrg.*, Vol. 31, pp. 1135~1149.

Dhatt, G., Gao, D. M. and Cheikh, A. B., 1990, "A Finite Element Simulations of Metal Flow in Moulds," *Int. J. Numer. Methods Engrg.*, Vol. 30, pp. 821~831.

Donea, J., Giuliani, S. and Laval, H., 1982, "Finite Element Solution of the Unsteady Navier-Stokes Equations by a Fractional Step Method," *Comput. Methods Appl. Mech. Engrg.*, Vol. 30, pp. 53~73.

Floryan, J. M. and Rasmussen, H., 1989, "Numerical Methods for Viscous Flows with Moving Boundaries," *Appl. Mech. Rev.*, Vol. 42, No. 12, pp. 323~341.

Gao, D. M., 1999, "A Three-Dimensional Hybrid Finite Element-Volume Tracking Model for Mould Filling in Casting Processes," *Int. J. Numer. Methods Fluids*, Vol. 29, pp. 877~895.

Gueyfier, D., Li, J., Nadim, A., Scardovelli, R. and Zaleski, S., 1999, "Volume-of-Fluid Interface Tracking with Smoothed Surface Stress Methods for Three-Dimensional Flows," *J. Comput. Phys.*, Vol. 152, pp. 423~456.

Harlow, F. H. and Welch, J. E., 1965, "Numerical Calculation of Time-Dependent Viscous Incompressible Flow of Fluid with Free Surface," *Physics of Fluids*, Vol. 8, No, 12, pp. 2182~2189.

Harvie, D. J. E. and Fletcher, D. F., 2000, "A New Volume of Fluid Advection Algorithm : The Stream Scheme," *J. Comput. Phys.*, Vol. 162, pp. 1~32.

Harvie, D. J. E. and Fletcher, D. F., 2001, "A New Volume of Fluid Advection Algorithm : the Defined Donating Region Scheme," *Int. J. Numer. Methods Fluids*, Vol. 35, pp. 151~172.

Hetu, J. F. and Ilinca, F., 1999, "A Finite Element Method for Casting Simulations," Numer. Heat Trans. Part A, Vol. 36, pp. 657~679.

Hirt, C. W. and Nichols, B. D., 1981, "Volume of Fluid(VOF) Method for the Dynamics of Free Boundaries," *J. Comput. Phys.*, Vol. 39, pp. 201~225.

Kawahara, M. and Ohmiya, K., 1985, "Finite Element Analysis of Density Flow using the Velocity Correction Method," *Int. J. Numer. Methods Fluids*, Vol. 5, pp. 981~993.

Kim, M. S., Shin, S. and Lee W. I., 2000, "A New VOF-based Numerical Scheme for the Simulation of Fluid Flow with Free Surface (I)-New Free Surface Tracking Algorithm and Its Verification," *Trans. of KSME (B)*, Vol. 24, pp. 1555~1569. (in Korean)

Kim, M. S., Park J. S. and Lee W. I., 2000, "A New VOF-based Numerical Scheme for the Simulation of Fluid Flow with Free Surface (II)-Application to the Cavity Filling and Sloshing Problems," *Trans. of KSME (B)*, Vol. 24, pp. 1570~1579. (in Korean)

Laval, H. and Quartapelle, L., 1990, "A Fractional-Step Taylor-Galerkin Method for Unsteady Incompressible Flows," *Int. J. Numer. Methods Fluids*, Vol. 11, pp. 501~513.

Lewis, R. W., Usmani, R. W. and Cross, J. T., 1995, "Efficient Mould Filling Simulation in Castings by an Explicit Finite Element Method," *Int. J. Numer. Methods Fluids*, Vol. 20, pp. 493~506.

Martin, J. C. and Moyce, W. J., 1952, "An Experimental Study of the Collapse of Liquid Columns on a Rigid Horizontal Plane," *Philos. Trans. Roy. Soc. London Serl A, Math. Phys. Sci.*, Vol. 244, pp. 312~324.

Mizukami, A. and Tsuchiya, M., 1984, "A Finite Element Method for the Three-Dimensional Non-Steady Navier-Stokes Equations," *Int. J. Numer. Methods Fluids*, Vol. 4, pp. 349~357.

Nakayama, T. and Mori, M., 1996, "An Eulerian Finite Element Method for Time-Dependent Free Surface Problems in Hydrodynamics," *Int. J. Numer. Methods Fluids*, Vol. 22, pp. 175~194.

Noh, W. F. and Woodward, P., 1976, "SLIC (Simple Line Interface Calculation)," in *Proceedings of the Fifth International Conference on Numerical Methods in Fluid Dynamis*, ed. van de Vooren, A. I. and Zandbergen, P. J., Lecture Notes in Physics, Vol. 59, pp. 330~340, Springer-Verlag, New York, USA.

Ramaswamy, B., 1988, "Finite Element Solution for Advection and Natural Convection Flows," *Computers & Fluids*, Vol. 16, pp. 349~388.

Ramaswamy, B. and Jue, T. C., 1992, "Some Recent Trends and Developments in Finite Element Analysis for Incompressible Thermal Flows," *Int. J. Numer. Methods Engrg.*, Vol. 35, pp. 671~707.

Ramshaw, J. D. and Trapp, J. A., 1976, "A Numerical Technique for Low-Speed Homogeneous Two-Phase Flow with Sharp Interface," *J. Comput. Phys.*, Vol. 21, pp. 438~453.

Rider, W. J. and Kothe, D. B., 1998, "Reconstructing Volume Tracking," *J. Comput. Phys.*, Vol. 141, pp. 112~152.

Rudman, M., 1997, "Volume-Tracking Methods for Interfacial Flow Calculations," *Int. J. Numer. Methods Fluids*, Vol. 24, pp. 671~691.

Scardovelli, R. and Zaleski, S., 1999, "Direct Numerical Simulation of Free-Surface and Interfacial Flow," *Annual Reviews Fluid Mechanics*, Vol. 31, pp. 567~603.

Shin, S. and Lee, W. I., 1997, "Finite Element Analysis of Flow with Moving Free Surface by Volume of Fluid Method," *Trans. of KSME (B)*, Vol. 21, No. 9, pp. 1230~1243. (in Korean)

Shin, S. and Lee, W. I., 2000, "Finite Element Analysis of Incompressible Viscous Flow with Moving Free Surface by Selective Volume of Fluid Method," *Int. J. Heat and Fluid Flow*,

Vol. 21, pp. 197~206.

Usmani, A. S., Cross, J. T. and Lewis, R. W., 1992, "A Finite Element Model for the Simulations of Mould Filling in Metal Casting and the Associated Heat Transfer," *Int. J. Numer. Methods Engrg.*, Vol. 35, pp. 787~806.

Young, D. L., 1982, "Time-Dependent Multi-Material Flow with Large Fluid Distortion," *in Numerical Methods for Fluid Dynamics*, ed. Morton, K. W. and Baines, M. J., pp. 273~285, Academic Press, New York.